A Model for Resource Competition in CRISPR-Mediated Gene Repression

Pin-Yi Chen, Yili Qian, and Domitilla Del Vecchio

***Abstract*—CRISPR-mediated gene regulation is known for its ability to control multiple targets simultaneously due to its modular nature: the same dCas9 effector can target different genes simply by changing the associated gRNA. However, multiplexing requires the sharing of limited amounts of dCas9 protein among multiple gRNAs, leading to resource competition. In turn, competition between gRNAs for the same resource may hamper network function. In this work, we develop a general model that takes into account the sharing of limited amounts of dCas9 protein for arbitrary CRISPR-mediated gene repression networks. We demonstrate that, as a result of resource competition, hidden interactions appear, which modifies the intended network regulations. As a case study, we analyze the effects of these hidden interactions on repression cascades. In particular, we illustrate that perfect adaptation to resource fluctuations can be achieved in cascades with an even number of repressors. In contrast, cascades with an odd number of repressors are substantially impacted by resource competition.**

I. INTRODUCTION

Synthetic genetic circuits have shown their potential in a number of applications, from energy, to environment, to medicine [1]. Effective and programmable synthetic transcription factors are the building blocks for complex and scalable synthetic circuits. CRISPR-Cas9 systems, one of the most exciting recent discoveries in biology, provide a simple and versatile tool for genetic modifications in various cell types and have been recently repurposed for transcriptional regulation [2]. Compared with other major classes of programmable synthetic transcription factors, such as ZFs [3], [4] and TALEs [5], CRISPR-mediated gene regulation offers unprecedented ease in multiplexing (i.e., regulating multiple genes simultaneously), which is vital for building complex gene circuits. The modular nature of this RNA-guided DNA recognition platform, where a single protein dCas9 can target different genes by changing the associated gRNA, makes RNA-guided transcriptional regulations precise and scalable.

Repression through CRISPR interface (CRISPRi) and activation through CRISPR-mediated gene activation (CRISPRa) have been achieved in diverse organisms, including bacterial and eukaryotic cells [6]. For CRISPRi in bacterial cells, by pairing dCas9 with sequence-specific sgRNAs, dCas9-sgRNA complexes can efficiently inhibit the transcription of targeted genes. In mammalian cells, CRISPRi can be enhanced by fusing dCas9 to a transcriptional repressor domain, such as KRAB [7] and SID4X [8]. In addition to CRISPRi, CRISPRa has been created by fusing dCas9 to ω-subunit [9] of RNA polymerase in bacteria. The fusion of transcriptional activators, such as VP64 and p65AD [7], to dCas9 leads to activation in mammalian cells. Simultaneous activation and repression of genes was also established by using scaffold RNAs (scRNAs) [10]. The scRNAs encode information both for DNA target recognition and for recruiting a specific repressor or activator protein. By sharing the same dCas9 protein, dCas9-scRNAs can simultaneously repress or activate multiple genes in the same cell (Fig. 1).

Previous work on building CRISPR-based circuits has demonstrated the potential of using CRISPR-mediated gene regulation to build layered, complex and scalable synthetic regulatory circuits [11]–[13]. However, as circuits become larger, a greater number of gRNAs are expressed, and thereby, competition for a finite pool of dCas9 may cause unintended interactions. In addition, since high levels of dCas9 concentration are toxic, leading to reduced cell growth [11], one cannot mitigate competition by arbitrarily increasing dCas9 production. Therefore, it is important to determine how competition for a finite amount of dCas9 affects the emergent circuit behavior.

The effects of resource competition have been extensively studied for different cellular resources, such as ribosomes [14] [15] and proteases [16] [17]. These studies demonstrated significant effects of resource competition and provided model-guided methodologies to minimize the resulting effects. However, to the best of our knowledge, there has not been any study about the effects of competition for dCas9 in CRISPR-based genetic circuits.

In this paper, we develop a simple ODE model whose state variables are the concentrations of the gRNAs and output proteins. The model, which explicitly accounts for the effects of dCas9 sharing, is general enough to capture arbitrary CRISPRi networks in both bacterial and mammalian cells. The steady state I/O responses are discussed in parallel networks, which do not contain regulations among gRNA. In addition, the "hidden" interactions, which are all activations for CRISPRi-based circuits, are added to the interaction graph of the system. Finally, the model is applied to CRISPR-based repression cascades and illustrates that even-stage cascades adapt better to the competition effect than odd-stage cascades under mild technical assumptions.

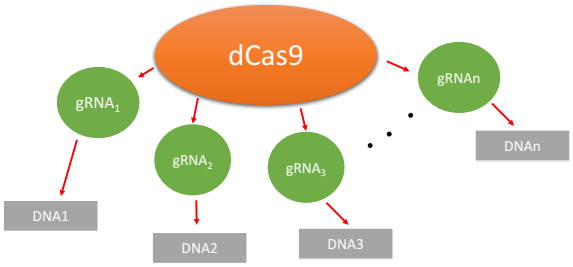

Fig. 1. dCas9 is the shared resource among multiple gRNAs.

This work was supported by AFOSR grant FA9550-14-1-0060.

P. -Y. Chen,Y. Qian and D. Del Vecchio are with the Department of Mechanical Engineering, MIT, Cambridge, MA 02139, USA. Emails: pinyi@mit.edu (P. -Y. Chen), yiliqian@mit.edu (Y. Qian) and ddv@mit.edu (D. Del Vecchio).

Preprint submitted to 57th IEEE Conference on Decision and Control.
Received March 15, 2018.

The rest of the paper is organized as follows. In Section II, we introduce the modeling framework for parallel repression networks and the concept of I/O response. In Section III, we introduce the general modeling framework, which is applicable to any repression-only network, such as repression cascades. Then, the concept of competition-induced hidden interactions is defined. In Section IV, an n-stage repression cascade example is detailed as an application of our general modeling framework. The design guideline for perfect adaptation to resource competition is provided.

II. RESOURCE COMPETITION IN PARALLEL NETWORKS

In this section, we focus on the parallel network, where there is no direct interactions between gRNAs.

A. Modeling Framework

There are a wide variety of CRISPR-based platforms for gene regulation. Both gRNA and dCas9 can be modified for a particular scenario, including repression or activation in bacterial or mammalian cells. In either case, there is always a pool of dCas9 or modified dCas9, such as dCas9-ω or dCas9-VP64, shared by sequence-specific gRNAs or scRNAs. Therefore, in this model, we neglect the conformational detail of each component, and lump the key species into two: the resource (dCas9 or modified dCas9) and the users (gRNAs or scRNAs), by naming them d and g, respectively. We first consider a network with n users without regulatory interactions among them (i.e., parallel network), which is shown in Fig. 2. For CRISPR-mediated gene regulation, d pairs with $\mathrm{g_i}$ ($i = 1, 2, \cdots, n$), forming dCas9-gRNA complexes ($\mathrm{c_i}$), which act as transcription factors. These transcription factors then interfere with the transcription elongation of the target genes ($\mathrm{D_i}$) to form complexes ($\mathrm{C_i}$):

$$\mathrm{d} + \mathrm{g_i} \underset{k_i^-}{\overset{k_i^+}{\rightleftharpoons}} \mathrm{c_i}, \qquad \mathrm{c_i} + \mathrm{D_i} \underset{q_i^-}{\overset{q_i^+}{\rightleftharpoons}} \mathrm{C_i}. \tag{1}$$

For CRISPR-mediated gene repression (CRISPRi), the free target genes ($\mathrm{D_i}$) are transcribed and then translated into output proteins ($\mathrm{Y_i}$). The concentrations of output proteins (Y_i) are used to study the repression level:

$$\mathrm{D_i} \xrightarrow{\kappa_i} \mathrm{Y_i} + \mathrm{D_i}. \tag{2}$$

For CRISPR-mediated gene activation (CRISPRa), the transcriptionally active complexes ($\mathrm{C_i}$) produce the output proteins ($\mathrm{Y_i}$):

$$\mathrm{C_i} \xrightarrow{\kappa_i} \mathrm{Y_i} + \mathrm{C_i}. \tag{3}$$

Independent of activation and repression, the resource sequestration mechanism can always be described by (1). For simplicity, we focus on CRISPRi for the remainder of this paper. The analysis of activation can be dealt with similarly and is left for future work. In our model, the decay (i.e., dilution and degradation) rates of the complexes (c_i and C_i) are neglected since we assume that k_i^- and q_i^- are much greater than the decay rate of complexes. The production rate of gRNA i is u_i. The decay rates of gRNAs and output proteins are δ and θ, respectively, which we assume to be constant for all nodes without loss of generality. We use d, g_i, c_i, C_i, D_i and Y_i to represent concentrations of species d, $\mathrm{g_i}$, $\mathrm{c_i}$, $\mathrm{C_i}$, $\mathrm{D_i}$ and $\mathrm{Y_i}$, respectively. Consequently, based on chemical reactions (1) - (2), we have the following ODE model from mass action kinetics:

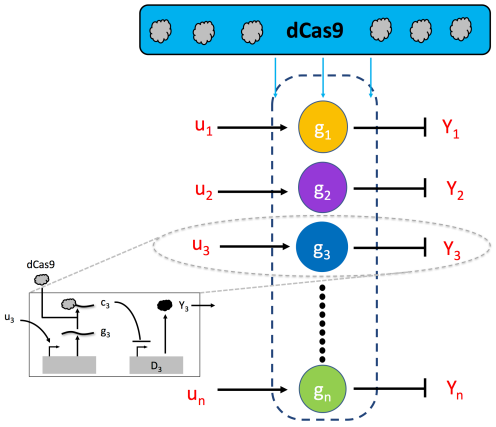

Fig. 2. A parallel network with n gRNAs

$$\dot{g}_i = u_i + k_i^- c_i - k_i^+ d g_i - \theta g_i, \tag{4}$$

$$\dot{c}_i = k_i^+ d g_i - k_i^- c_i + q_i^- C_i - q_i^+ c_i D_i, \tag{5}$$

$$\dot{C}_i = q_i^+ c_i D_i - q_i^- C_i, \tag{6}$$

$$\dot{Y}_i = \kappa_i D_i - \delta Y_i, \tag{7}$$

Since dCas9 is produced constitutively, the total concentration of dCas9 (d_t) is conserved ($d_t = \alpha_d/\delta$, where α_d is the production rate of dCas9). The total concentrations of DNAs are conserved as well [18]. Therefore, we have

$$d_t = d + \sum_{i=1}^{n} c_i + \sum_{i=1}^{n} C_i, \tag{8}$$

$$D_{it} = D_i + C_i, \tag{9}$$

where D_{it} is the total concentrations of $\mathrm{D_i}$. Since the binding reactions in (1) are much faster than the production and decay of proteins and RNAs [19], the time derivatives in equations (5) and (6) are set to zero (quasi-steady state assumption). The complex concentrations in each node i at quasi-steady state (QSS) are as follows:

$$c_i = \frac{d g_i}{K_i}, \quad C_i = \frac{d g_i D_i}{K_i Q_i}, \tag{10}$$

where dissociation constants K_i and Q_i are defined as:

$$K_i = \frac{k_i^-}{k_i^+}, \quad Q_i = \frac{q_i^-}{q_i^+}.$$

From (9) and (10), free DNA concentration (D_i) at steady state can be written as:

$$D_i = \frac{D_{it}}{1 + \frac{d g_i}{K_i Q_i}}. \tag{11}$$

To obtain the free dCas9 concentration d, we substitute (10) and (11) into equation (8) to obtain:

$$F(d, \mathbf{g}) := d\left(1 + \sum_{i=1}^{n} \frac{g_i}{K_i}\right) + \sum_{i=1}^{n} \frac{d g_i D_{it}}{K_i Q_i + d g_i} - d_t = 0, \tag{12}$$

where we use vector $\mathbf{g} := [g_1, \cdots, g_n]^T$ to represent all gRNA concentrations in the system. For any given $\mathbf{g}$, since $F(\mathbf{g}, d)$ is monotonically increasing with d for all $d > 0$ and ranges $(-d_t, +\infty)$, equation (12) has a unique positive solution $d = d(\mathbf{g}) > 0$. By substituting c_i concentrations from

Preprint submitted to 57th IEEE Conference on Decision and Control.
Received March 15, 2018.

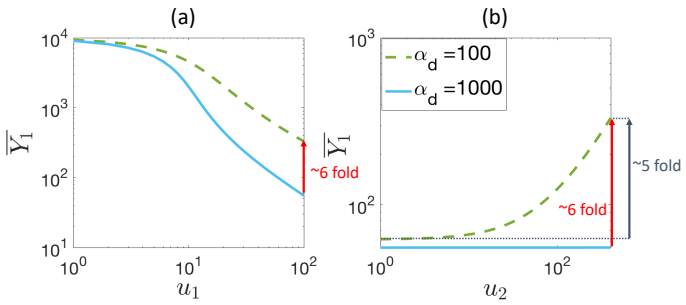

Fig. 3. I/O steady state response of a parallel network with two gRNAs. The red lines in both figures represent the fold change of $\bar{Y}_1$ concentration from the case with abundant resources ($\alpha_d = 1000\text{nMhr}^{-1}$) to that with limited resources ($\alpha_d = 100\text{nMhr}^{-1}$) when $u_1 = 100\text{nMhr}^{-1}$ and $u_2 = 400\text{nMhr}^{-1}$. The black line in the right figure represents the fold change ("hidden activation") from $u_2 = 0\text{nMhr}^{-1}$ to $u_2 = 400\text{nMhr}^{-1}$ when $\alpha_d = 100\text{nMhr}^{-1}$. In the left figure, u_2 concentration is fixed at 400nMhr^{-1}. In the right figure, u_1 concentration is fixed at 100nMhr^{-1}. Other Parameters: $D_{1t} = D_{2t} = 10\text{nM}$, $K_1 = K_2 = 0.01\text{nM}$ [20], $Q_1 = Q_2 = 0.5\text{nM}$ [21], $\delta = 1\text{hr}^{-1}$, $\theta = 100\text{hr}^{-1}$, $\kappa = 1000\text{hr}^{-1}$.

(10) into (4) and by substituting free DNA concentration (11) into (7), the dynamics of (4)-(7) become:

$$\dot{g}_i = u_i - \theta g_i, \tag{13}$$

$$\dot{Y}_i = \frac{\beta_i}{1 + d(\mathbf{g}) g_i/\lambda_i} - \delta Y_i. \tag{14}$$

where $\lambda_i := K_i Q_i$ and $\beta_i := \kappa_i D_{it}$. The above equations show that gRNA's dynamics (13) depend only on the inputs. The competition effect is captured in (14), where the steady state free dCas9 concentration $\bar{d}$ is a function of gRNA concentrations $\mathbf{g}$ and appears in the denominator. For a constant input u_i, steady state gRNA concentrations $\bar{g}_i$ and output protein concentrations $\bar{Y}_i$ can be computed from (13)-(14):

$$\bar{g}_i = \frac{u_i}{\theta}, \quad \bar{Y}_i = \frac{\beta_i'}{1 + \bar{d}(\mathbf{g})\bar{g}_i/\lambda_i}, \quad \text{where} \quad \beta_i' := \frac{\beta_i}{\delta}. \tag{15}$$

When there are abundant resources, dCas9 concentration remains approximately constant, $\bar{d} \approx d_t$. In this case the output concentrations at steady state $\bar{Y}_i$ can be written as:

$$\bar{Y}_i = \frac{\beta_i'}{1 + d_t \bar{g}_i/\lambda_i}, \quad \text{where} \quad \beta_i' = \frac{\beta_i}{\delta}.$$

We perform numerical simulations on a two-gRNA parallel network based on (13)-(14) we derived as an illustrative example (Fig. 3). As the production rate (α_d) of dCas9 decreases, the intended regulation effect is altered. In Fig. 3 (a), when the production rate of the resource decreases by 10-fold, the repression level diminishes by approximately 6-fold (the red line in 3 (a)). In Fig. 3 (b), the input u_2 is essentially uncoupled with Y_1 when there are sufficient resources (the blue line). When the production of resource decreases by 10-fold, the "hidden activation" from u_2 to Y_1 becomes appreciable (about 5-fold). The diminished repression level and hidden activation level depend not only on the amount of gRNAs (u_1, u_2) and dCas9 (α_d) but also on other parameters, such as dissociation constants (K_1, K_2, Q_1, Q_2), dilution rates (θ, δ), the amount of targets (D_{1t}, D_{2t}), and the output promoter strengths (κ_1). The parameters used in the simulation are estimated from literature [20]–[22] and preliminary experimental results.

B. Conservation of dCas9

In the following section, the relation between the free amount of dCas9 (d) and gRNA concentrations ($\mathbf{g}$) is studied base on equation (12). First, we consider two extreme scenarios to explicitly represent d as a function of $\mathbf{g}$. Then, we investigate how d changes qualitatively with $\mathbf{g}$, namely, $\partial d/\partial g_i$. This information will be utilized later when we evaluate the sign of the I/O response and the interaction graph.

Scenario (i): High Repression Level

When there are sufficient dCas9 and gRNAs in the system, abundant repressors are formed. Under this scenario, all the targets are repressed, namely, the amount of repressed targets approximately equals the total amount of targets: $C_i \approx D_{it}$. Equation (8) can be written as:

$$d_t = d + \sum_{i=1}^{n} c_i + \sum_{i=1}^{n} D_{it}. \tag{16}$$

By substituting equation (10) into the above equation, we obtain the free dCas9 concentration:

$$d = d(\mathbf{g}) = \frac{d_t - \sum_{i=1}^{n} D_{it}}{1 + \sum_{i=1}^{n} \frac{g_i}{K_i}}. \tag{17}$$

Scenario (ii): Low Repression Level

When there are limited dCas9 protein or gRNAs, most targets are not being repressed. Under this scenario, the amount of free DNAs approximately equals the total amount of DNAs: $D_i \approx D_{it}$. By substituting (10) into equation (8), we obtain:

$$d_t = d + \sum_{i=1}^{n} c_i + \sum_{i=1}^{n} \frac{d g_i D_i}{K_i Q_i}.$$

By substituting equation (10) into the above equation, we obtain the free dCas9 concentration:

$$d = d(\mathbf{g}) = \frac{d_t}{1 + \sum_{i=1}^{n} \frac{g_i}{K_i} + \sum_{i=1}^{n} \frac{g_i D_{it}}{K_i Q_i}}.$$

Next, we investigate the sign of $\partial d/\partial g_i$. Since $\partial F/\partial d \neq 0$ for all $d > 0$ in (12), by the implicit function theorem [23], we have:

$$\frac{\partial d}{\partial g_i} = -\frac{\partial F/\partial g_i}{\partial F/\partial d}. \tag{18}$$

We explicitly find the sign of $\partial F/\partial g_i$ and $\partial F/\partial d$:

$$\frac{\partial F}{\partial g_i} = \frac{d}{K_i} + \frac{d D_{it} K_i Q_i}{(K_i Q_i + d g_i)^2} > 0, \tag{19a}$$

$$\frac{\partial F}{\partial d} = 1 + \sum_{i=1}^{n} \frac{g_i}{K_i} + \sum_{i=1}^{n} \frac{g_i D_{it} K_i Q_i}{(K_i Q_i + d g_i)^2} > 0. \tag{19b}$$

Consequently, according to (18), the sign of $\partial d/\partial g_i$ is guaranteed to be negative (i.e., $\text{sign}[\partial d/\partial g_i] < 0$, $\forall i$).

C. Steady State I/O Response

The steady state I/O response reflects the competition effect when resource is limited. The following equation describes the steady state I/O response from any input u_j to

Preprint submitted to 57th IEEE Conference on Decision and Control.
Received March 15, 2018.

any output $\bar{Y}_i$ in a parallel network:

$$\frac{\partial \bar{Y}_i}{\partial u_j} = \overbrace{\underbrace{\frac{\partial \bar{Y}_i}{\partial \bar{g}_j}\cdot\frac{\partial \bar{g}_j}{\partial u_j}}_{\text{negative}}}^{S,\text{ intended regulatory effect}} + \overbrace{\underbrace{\frac{\partial \bar{Y}_i}{\partial \bar{d}}\cdot\frac{\partial \bar{d}}{\partial \bar{g}_j}\cdot\frac{\partial \bar{g}_j}{\partial u_j}}_{\text{positive}}}^{C,\text{ competition effect}}.$$

The first term (S) is due to the intended regulation (i.e. repression), and the second term (C) arises from unintended interactions due to resource competition.

***Claim** 1:* The steady state I/O response of the parallel network in (15) satisfies:

$$\frac{\partial \bar{Y}_i}{\partial u_j} < 0 \text{ if } i = j, \qquad \frac{\partial \bar{Y}_i}{\partial u_j} > 0 \text{ otherwise.}$$

Proof: At steady state, $d = \bar{d}$, $g_i = \bar{g}_i$, from equation (15), (18) and (19), when $i = j$, we have:

$$\frac{\partial \bar{Y}_i}{\partial \bar{g}_i} = -\frac{\beta_i \bar{d}}{(1+\bar{d}\bar{g}_i/\lambda_i)^2}.$$

$$\frac{\partial \bar{Y}_i}{\partial \bar{d}}\cdot\frac{\partial \bar{d}}{\partial \bar{g}_i} = -\frac{\beta_i \bar{g}_i}{(1+\bar{d}\bar{g}_i/\lambda_i)^2}\cdot\frac{-\bar{d}}{\bar{g}_i}\cdot R,$$

$$\text{where} \quad R = \frac{\frac{\bar{g}_i}{K_i} + \frac{\bar{g}_i D_{it} K_i Q_i}{(K_i Q_i + d\bar{g}_i)^2}}{1 + \sum_{i=1}^n \frac{\bar{g}_i}{K_i} + \sum_{i=1}^n \frac{\bar{g}_i D_{it} K_i Q_i}{(K_i Q_i + d\bar{g}_i)^2}} < 1.$$

Therefore,

$$\frac{\partial \bar{Y}_i}{\partial \bar{g}_i} + \frac{\partial \bar{Y}_i}{\partial \bar{d}}\cdot\frac{\partial \bar{d}}{\partial \bar{g}_i} < 0.$$

Since $\partial \bar{g}_i/\partial u_i > 0$, we have:

$$\frac{\partial \bar{Y}_i}{\partial u_i} = \left(\frac{\partial \bar{Y}_i}{\partial \bar{g}_i} + \frac{\partial \bar{Y}_i}{\partial \bar{d}}\cdot\frac{\partial \bar{d}}{\partial \bar{g}_i}\right)\cdot\frac{\partial \bar{g}_i}{\partial u_i} < 0.$$

When $i \neq j$, we have:

$$\frac{\partial \bar{Y}_i}{\partial u_j} = 0 + \underbrace{\frac{\partial \bar{Y}_i}{\partial \bar{d}}}_{\text{negative}}\cdot\underbrace{\frac{\partial \bar{d}}{\partial \bar{g}_j}}_{\text{negative}}\cdot\underbrace{\frac{\partial \bar{g}_j}{\partial u_j}}_{\text{positive}} > 0.$$

■

***Remark** 1:* The claim above implies that while resource competition and intended regulation always have opposite signs, the resource competition effect is always weaker when $i = j$. When $i \neq j$, there is no intended interaction, and resource competition always causes hidden activation.

In practice, when repressing multiple targets, another simple and common experimental setting is to have a single inducer u regulating the production of multiple gRNAs (Fig. 4). Under this scenario, one input controls multiple outputs. The following claim shows that the intended regulation (i.e., repression) remains qualitatively unchanged in the presence of competition.

***Claim** 2:* When $u = u_1 = u_2 = \cdots = u_n$, the steady state response of (15) satisfies:

$$\frac{\mathrm{d}\bar{Y}_j}{\mathrm{d}u} < 0 \quad \forall j.$$

TABLE I. THREE TYPES OF NODES IN A CRISPRI GENE REGULATION CIRCUIT

type	1	2	3
input	external inducer	dCas9-gRNA	dCas9-gRNA
output	dCas9-gRNA	dCas9-gRNA	protein

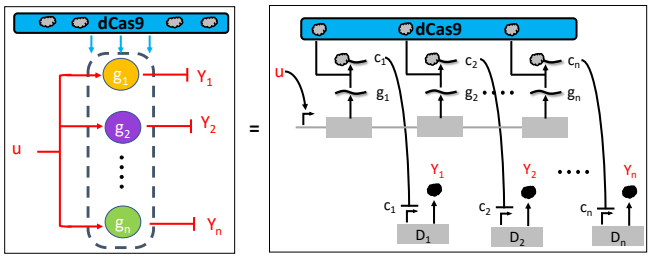

Fig. 4. A parallel network controlled by a single input with n outputs

Proof:

$$\frac{\mathrm{d}\bar{Y}_j}{\mathrm{d}u} = \underbrace{\frac{\partial \bar{Y}_j}{\partial \bar{d}}\cdot\left(\sum_{i=1}^n \frac{\partial \bar{d}}{\partial \bar{g}_i}\frac{\mathrm{d}\bar{g}_i}{\mathrm{d}u}\right)}_{\text{C, competition effect}} + \underbrace{\frac{\partial \bar{Y}_j}{\partial \bar{g}_j}\cdot\frac{\mathrm{d}\bar{g}_j}{\mathrm{d}u}}_{\text{S, intended regulatory effect}}$$

$$= \frac{\beta_j \bar{d}}{(1+\bar{d}\bar{g}_j/\lambda_j)^2}\cdot\theta\cdot(R-1),$$

$$\text{where} \quad R = \frac{\sum_{i=1}^n \frac{\bar{g}_j}{K_i} + \frac{\bar{g}_j D_{it} K_i Q_i}{(K_i Q_i + d\bar{g}_i)^2}}{1 + \sum_{i=1}^n \frac{\bar{g}_i}{K_i} + \sum_{i=1}^n \frac{\bar{g}_i D_{it} K_i Q_i}{(K_i Q_i + d\bar{g}_i)^2}}.$$

Since $u = u_1 = u_2 = \cdots = u_n$, we must have $\bar{g}_1 = \cdots = \bar{g}_n$, this results in $R < 1$. Consequently, $\mathrm{d}\bar{Y}_j/\mathrm{d}u < 0$.

■

III. RESOURCE COMPETITION IN GENERAL NETWORKS

Complex CRISPRi networks may have direct regulations between gRNAs (i.e. the repressors formed by one gRNA and dCas9 repress the production of another gRNA in the network). Therefore, in this section, we provide a general modeling framework that captures arbitrary CRISPRi networks. Here, we first give a high-level description of a CRISPRi gene regulation network in Section III-A, which includes a classification of 3 types of nodes in the network. We then describe the dynamics in each type of nodes (Section III-B) and introduce the resource constraint imposed on the network (Section III-C). We summarize the network resource competition model in Section III-D. We demonstrate in Section III-E how resource competition gives rise to hidden interactions among nodes.

A. Preliminaries

We consider a CRISPRi network composed of m nodes. Depending on the biomolecular species, each node takes as input and produces as output, they can be classified into 3 types which are shown in Table I (see also Fig. 5). We use index sets $\mathcal{I}_1$, $\mathcal{I}_2$ and $\mathcal{I}_3$ to denote the set of nodes that fall into type 1,2 and 3, respectively, and define $\mathcal{I} := \bigcup_{i=1}^3 \mathcal{I}_i = \{1, \cdots, m\}$. In a type 1 (2) node, an external inducer (a set of dCas9-gRNA complexes) regulates the transcription of a gRNA, which can bind with dCas9 to form a dCas9-gRNA complex as an output. In contrast, a type 3 node is regulated by a set of dCas9-gRNA complexes to produce protein as outputs. We let $\mathcal{I}_1 = \{1, \cdots r\}$, $\mathcal{I}_2 = \{r+1, \cdots, r+p\}$ and $\mathcal{I}_3 = \{r+p+1, \cdots, r+p+l\}$. Vector $\mathbf{Y} \in \mathbb{R}^l$ represents the concatenations of output proteins in $\mathcal{I}_3$. We also let $n := |\mathcal{I}_1 \cup \mathcal{I}_2| = r + p$. Vector $\mathbf{g} \in \mathbb{R}^n$ represents the gRNA

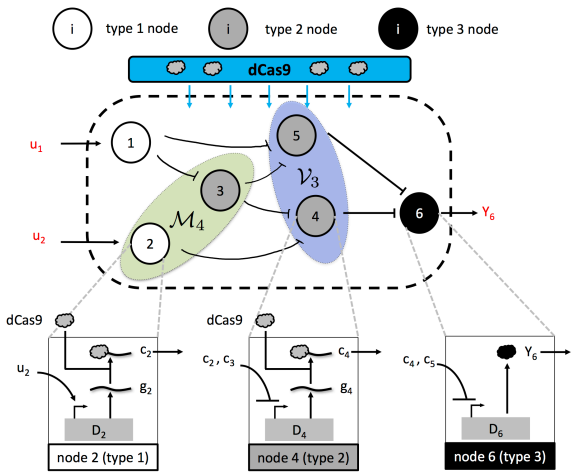

Fig. 5. An example CRISPRi regulation network. This network can be modeled by the general modeling framework. It is composed of 6 nodes. Nodes of type 1, 2 and 3 are colored white, gray and black respectively. Biomolecular processes for node 2, 4 and 6 are shown as examples. The set of parent nodes to node 4 is $\mathcal{M}_4 = \{2, 3\}$ and the set of target nodes of node 3 is $\mathcal{V}_3 = \{4, 5\}$.

concentrations in $\mathcal{I}_1$ and $\mathcal{I}_2$. We use $\mathcal{V}_i \subseteq \mathcal{I} \setminus \mathcal{I}_1$ to represent the set of nodes regulated by node i (i.e., *targets* of node i). Similarly, we use $\mathcal{M}_i \subseteq \mathcal{I} \setminus \mathcal{I}_3$ to represent the set of nodes that regulate the transcription in node i (i.e., *parents* of node i). We use vector $\check{\mathbf{g}}_i \in \mathbb{R}^{|\mathcal{M}_i|}$ to represent the concatenation of gRNA concentrations in $\mathcal{M}_i$. An example network with $m = 6$ nodes is shown in Fig. 5. In this example, nodes of different types are filled with different colors. Specifically, we have $\mathcal{I}_1 = \{1, 2\}$, $\mathcal{I}_2 = \{3, 4, 5\}$ and $\mathcal{I}_3 = \{6\}$. As an illustrative example, the set of parents to node 4 is $\mathcal{M}_4 = \{2, 3\}$, and therefore, $\check{\mathbf{g}}_4 = [g_2, g_3]^T$. The set of targets of node 3 is $\mathcal{V}_3 = \{4, 5\}$.

In what follows, we describe in detail the chemical reactions and dynamics in each type of node.

B. Dynamics in a node

1) Type 1 node: A type 1 node $i \in \mathcal{I}_1$ takes an external inducer $\mathrm{u_i}$ as input to produce a gRNA $\mathrm{g_i}$, which binds with free dCas9 (d) in the network to form an active regulatory complex $\mathrm{c_i}$ as outputs. These chemical reactions can be written as:

$$\emptyset \xrightarrow{\mathrm{u_i}} \mathrm{g_i}, \quad \mathrm{g_i} \xrightarrow{\theta} \emptyset, \quad \mathrm{d} + \mathrm{g_i} \underset{k_i^-}{\overset{k_i^+}{\rightleftharpoons}} \mathrm{c_i}.$$

The output complex $\mathrm{c_i}$ can then bind with DNA of its target node $k \in \mathcal{V}_i$, D_k, to repress its transcription:

$$\mathrm{D_k} + \mathrm{c_i} \underset{q_{ik}^-}{\overset{q_{ik}^+}{\rightleftharpoons}} \mathrm{C_{ik}}, \quad \forall k \in \mathcal{V}_i.$$

Based on the above chemical reactions, the dynamics of g_i and c_i in node i follow:

$$\dot{g}_i = u_i - \theta g_i + k_i^- c_i - k_i^+ d g_i, \tag{20a}$$

$$\dot{c}_i = k_i^+ d g_i - k_i^- c_i + \sum_{k \in \mathcal{V}_i} (q_{ik}^- C_{ik} - q_{ik}^+ c_i D_k). \tag{20b}$$

2) Type 2 node: The transcription of gRNA g_i from its DNA D_i in a type 2 node $i \in \mathcal{I}_2$ is repressed by a set of dCas9-gRNA complexes produced by its parents, resulting in the following chemical reactions for each $j \in \mathcal{M}_i$:

$$\mathrm{c_j} + \mathrm{D_i} \underset{q_{ji}^-}{\overset{q_{ji}^+}{\rightleftharpoons}} \mathrm{C_{ji}}, \qquad \mathrm{D_i} \xrightarrow{\kappa_i} \mathrm{D_i} + \mathrm{g_i},$$

$$\mathrm{d} + \mathrm{g_i} \underset{k_i^-}{\overset{k_i^+}{\rightleftharpoons}} \mathrm{c_i}, \qquad \mathrm{g_i} \xrightarrow{\theta} \emptyset.$$

The output $\mathrm{c_i}$ can then repress a target node $k \in \mathcal{V}_i$ by binding to its DNA D_k to block transcription:

$$\mathrm{D_k} + \mathrm{c_i} \underset{q_{ik}^-}{\overset{q_{ik}^+}{\rightleftharpoons}} \mathrm{C_{ik}}, \quad \forall k \in \mathcal{V}_i.$$

Based on these reactions, the dynamics of C_{ji}, g_i and c_i can be written as:

$$\dot{C_{ji}} = q_{ji}^+ c_j D_i - q_{ji}^- C_{ji}, \tag{21a}$$

$$\dot{g}_i = \kappa_i D_i - \theta g_i + k_i^- c_i - k_i^+ d g_i, \tag{21b}$$

$$\dot{c}_i = k_i^+ d g_i - k_i^- c_i + \sum_{k \in \mathcal{V}_i} (q_{ik}^- C_{ik} - q_{ik}^+ c_i D_k). \tag{21c}$$

3) Type 3 node: A node $i \in \mathcal{I}_3$ is repressed by its parent nodes to express a protein Y_i from its DNA D_i as outputs. In particular, dCas9-gRNA complexes c_j produced by any node $j \in \mathcal{M}_i$ can block the transcription of Y_i. We assume that when he production of Y_i is not repressed, it takes place with a constant rate κ_i. These processes can be described by the following chemical reactions:

$$\mathrm{c_j} + \mathrm{D_i} \underset{q_{ji}^-}{\overset{q_{ji}^+}{\rightleftharpoons}} \mathrm{C_{ji}}, \quad \mathrm{D_i} \xrightarrow{\kappa_i} \mathrm{D_i} + \mathrm{Y_i}, \quad \mathrm{Y_i} \xrightarrow{\delta} \emptyset,$$

where δ is the decay rate constant. These reactions can be described by the following ODEs:

$$\dot{C_{ji}} = q_{ji}^+ c_j D_i - q_{ji}^- C_{ji}, \tag{22a}$$

$$\dot{Y_i} = \kappa_i D_i - \delta Y_i. \tag{22b}$$

Now that we have studied the dynamics in all types of nodes, we are ready to factor resource competition into the model.

C. Conservation of dCas9

We assume that the circuit produces a limited amount of dCas9 (d_t) available to all nodes, and therefore follows the conservation law:

$$d_t = d + \sum_{i \in \mathcal{I} \setminus \mathcal{I}_3} c_i + \sum_{i \in \mathcal{I} \setminus \mathcal{I}_3} \sum_{j \in \mathcal{V}_i} C_{ij}, \tag{23}$$

where we have summed up dCas9 as follows: 1) Those bound to form DNA-dCas9-gRNA complexes (C_{ij}), which only appears in type 2 and 3 nodes. 2) Those bound to form dCas9-gRNA complexes c_i, which only appears in type 1 and 2 nodes.

Assuming that binding reactions are much faster than the transcription, we can compute the QSS concentrations of C_{ij} and c_i. Specifically, by setting the time derivatives in equations (21a) and (22a) to 0, we find that

$$C_{ij} = \frac{c_i D_j}{Q_{ij}}, \quad \forall i \in \mathcal{I} \setminus \mathcal{I}_3, \ j \in \mathcal{V}_i. \tag{24}$$

Note that in (20b) and (21c), for any $k \in \mathcal{V}_i \subseteq \mathcal{I} \setminus \mathcal{I}_1$, we must have $i \in \mathcal{M}_k$. Therefore, we can substitute the result in (24) into (20b) and (21c), and find c_i at QSS by setting the time derivatives to 0 in (20b) and (21c) to obtain

$$c_i = \frac{d g_i}{K_i}, \quad \forall i \in \mathcal{I} \setminus \mathcal{I}_3. \tag{25}$$

Preprint submitted to 57th IEEE Conference on Decision and Control.
Received March 15, 2018.

Substituting the results in (24) and (25) into the conservation law (23), we obtain:

$$d_t = d\left[1 + \sum_{i\in\mathcal{I}\setminus\mathcal{I}_3} \frac{g_i}{K_i} + \sum_{i\in\mathcal{I}\setminus\mathcal{I}_3}\sum_{j\in\mathcal{V}_i} \frac{g_i D_j}{K_i Q_{ij}}\right]. \quad (26)$$

To find the free DNA concentration D_i in (26), we assume that the total concentration of DNA D_{it} in any node $i \in \mathcal{I}\setminus\mathcal{I}_1$ is conserved [18]:

$$D_{it} = D_i + \sum_{j\in\mathcal{M}_i} C_{ji} = D_i\left[1 + d\sum_{j\in\mathcal{M}_i} \frac{g_j}{Q_{ji}K_i}\right], \quad (27)$$

where we have substituted in the results in equations (24) and (25). To find free dCas9 amount, we use equations (26) and (27) and then obtain:

$$F(d,\mathbf{g}) := d(1 + \sum_{i\in\mathcal{I}\setminus\mathcal{I}_3} \frac{g_i}{K_i}) + \sum_{i\in\mathcal{I}\setminus\mathcal{I}_3}\sum_{j\in\mathcal{V}_i} \frac{dg_i D_{jt}}{K_i Q_{ij}(1 + d\sum_{k\in\mathcal{M}_j} \frac{g_k}{K_k Q_{kj}})} - d_t = 0. \quad (28)$$

For any given $\mathbf{g}$, since $F(\mathbf{g}, d)$ is monotonically increasing with d for all $d > 0$ and ranges $(-d_t, +\infty)$, equation (28) has a unique positive solution $d = d(\mathbf{g}) > 0$. In the following section, the relation between the free amount of dCas9 (d) and gRNA concentrations ($\mathbf{g}$) is studied similarly to that of the parallel network in Section II. First, we consider two extreme scenarios. Then, we investigate $\partial d/\partial g_i$ qualitatively for more general situations.

Scenario (i): High Repression Level

When there are sufficient dCas9 and gRNAs in the system, abundant repressors are formed. Under this scenario, all the targets are repressed, namely, the number of repressed targets approximately equals to the total number of targets: $\sum_{j\in\mathcal{M}_i} C_{ji} \approx D_{it}$. Equation (23) can be written as:

$$d_t = d + \sum_{i\in\mathcal{I}\setminus\mathcal{I}_3} c_i + \sum_{i\in\mathcal{I}\setminus\mathcal{I}_1} D_{it}. \quad (29)$$

By substituting equation (10), we solve for free dCas9 concentration:

$$d = d(\mathbf{g}) = \frac{d_t - \sum_{i\in\mathcal{I}\setminus\mathcal{I}_1} D_{it}}{1 + \sum_{i\in\mathcal{I}\setminus\mathcal{I}_3} \frac{g_i}{K_i}}, \quad (30)$$

where $\mathbf{g} = [g_1, g_2, \cdots, g_n]$.

Scenario (ii): Low Repression Level

When there are limited dCas9 protein or gRNAs, most targets are not being repressed. Under this scenario, the number of free DNAs is approximately equal to the total number of DNAs: $D_i \approx D_{it}$. Equation (23) can be written as:

$$d_t = d + \sum_{i\in\mathcal{I}\setminus\mathcal{I}_3} c_i + \sum_{i\in\mathcal{I}\setminus\mathcal{I}_3}\sum_{j\in\mathcal{V}_i} \frac{dg_i D_{jt}}{K_i Q_{ij}}.$$

Next, we apply (10) to solve for free dCas9 concentration:

$$d = d(\mathbf{g}) = \frac{d_t}{1 + \sum_{i\in\mathcal{I}\setminus\mathcal{I}_3} \frac{g_i}{K_i} + \sum_{i\in\mathcal{I}\setminus\mathcal{I}_3}\sum_{j\in\mathcal{V}_i} \frac{g_i D_{jt}}{K_i Q_{ij}}}.$$

Finally, we focus on deriving the sign of $\partial d/\partial g_i$ for the most general cases. From (28), we have:

$$\frac{\partial F}{\partial d} = 1 + \sum_{i=1}^{n} \frac{g_i}{K_i} + \sum_{i\in\mathcal{I}\setminus\mathcal{I}_3}\sum_{j\in\mathcal{V}_i} \frac{g_i D_{jt} K_i Q_{ij}}{[K_i Q_{ij}(1 + d\sum_{k\in\mathcal{M}_j} \frac{g_k}{K_k Q_{kj}})]^2} > 0,$$

$$\frac{\partial F}{\partial g_i} = \frac{d}{K_i} + \sum_{j\in\mathcal{V}_i} \frac{d D_{jt} K_i Q_{ij}}{[K_i Q_{ij}(1 + d\sum_{k\in\mathcal{M}_j} \frac{g_k}{K_k Q_{kj}})]^2} > 0.$$

Since $\partial F/\partial d \neq 0$ for all positive d, by the implicit function theorem, we have:

$$\frac{\partial d}{\partial g_i} = -\frac{\partial F/\partial g_i}{\partial F/\partial d} < 0. \quad \forall i = 1, 2, \cdots, n \quad (31)$$

Consequently, the sign of the derivative $\partial d/\partial g_i$ is also guaranteed to be negative in a general network. This result will later be used to explore the sign of the *competition-induced hidden interaction* in Section III-E.

D. Summary

Since the dynamics of complexes C_{ij} and c_i have been set to QSS in all nodes, node dynamics can be reduced to that of the gRNAs and the protein. Therefore, from equations (20a), (21b), (22b) and the free DNA concentration obtained in (27), the dynamics in each type of node becomes:

$$\dot{g_i} = u_i - \theta g_i, \qquad \forall i \in \mathcal{I}_1, \quad (32a)$$

$$\dot{g_i} = \kappa_i D_i - \theta g_i, \qquad \forall i \in \mathcal{I}_2, \quad (32b)$$

$$\dot{Y_i} = \kappa_i D_i - \delta Y_i, \qquad \forall i \in \mathcal{I}_3. \quad (32c)$$

Using the results in (27), we can find the free DNA concentration D_i to substitute into (32) to yield:

$$\dot{g_i} = u_i - \theta g_i, \qquad \forall i \in \mathcal{I}_1, \quad (33a)$$

$$\dot{g_i} = \frac{\beta_i}{1 + d(\mathbf{g})G_i(\check{\mathbf{g}}_i)} - \theta g_i, \qquad \forall i \in \mathcal{I}_2, \quad (33b)$$

$$\dot{Y_i} = \frac{\beta_i}{1 + d(\mathbf{g})G_i(\check{\mathbf{g}}_i)} - \delta Y_i, \qquad \forall i \in \mathcal{I}_3, \quad (33c)$$

where we have defined

$$G_i(\check{\mathbf{g}}_\mathbf{i}) := \sum_{j\in\mathcal{M}_i} \frac{g_j}{\lambda_{ji}}, \quad \beta_i := \kappa_i D_{it}, \quad \text{and} \quad \lambda_{ji} := K_j Q_{ji}.$$

E. Competition-Induced Hidden Interactions

In this section, we explore the question: how does competition effect alter the intended interactions in a general network? We start by stacking the overall system dynamics from equation (33) to obtain the dynamics of the entire network:

$$\dot{\mathbf{x}} = \mathbf{F}(\mathbf{x}, \mathbf{u}) = \mathbf{f}(\mathbf{x}, d(\mathbf{x}), \mathbf{u}), \quad (34)$$

where $\mathbf{x} = [\mathbf{g}, \mathbf{Y}]^T$ is a vector composed of the states of all nodes in the network. By this definition, the states in vector $\mathbf{x}$ belong to those of the type 1-3 nodes, successively. Let the Jacobian matrix of $\mathbf{F}$ be:

$$\frac{\partial \mathbf{F}}{\partial \mathbf{x}} = \underbrace{\frac{\partial \mathbf{f}}{\partial \mathbf{x}}}_{\text{A}} + \underbrace{\frac{\partial \mathbf{f}}{\partial d} \cdot \frac{\partial d}{\partial \mathbf{x}}}_{\text{E}}. \quad (35)$$

Matrix A represents the intended regulatory interactions. When there are direct regulations from node i to node j, entry a_{ij} is nonzero; when there are no direct regulations, entry a_{ij} is zero. Matrix E represents the competition effect. Since matrix E stems from the dependence of f on d,

Preprint submitted to 57th IEEE Conference on Decision and Control.
Received March 15, 2018.

every nonzero entry e_{ij} in E captures how dynamics of x_i is affected by x_j through resource competition. Based on this, we introduce the notion of *competition-induced hidden interaction*. In general, e_{ij} is nonzero only when x_i represents either a gRNA produced by a type 2 node ($x_i = g_i, i \in \mathcal{I}_2$) or a protein ($x_i = Y_i, i \in \mathcal{I}_3$), and x_j is a gRNA ($x_j = g_j, j \in \mathcal{I} \setminus \mathcal{I}_3$).

Definition We define the hidden interaction $C(x_i, x_j)$ as:

$$C(x_i, x_j) := e_{ij} = \frac{\partial f_i}{\partial d} \cdot \frac{\partial d}{\partial x_j}, \tag{36}$$

where e_{ij} is the entry in the i-th row and j-th column of matrix E. When $C(x_i, x_j) = 0$, we say that there is no competition-induced hidden interaction from x_j to x_i. When $C(x_i, x_j) > 0 (< 0)$, there is a hidden activation (repression) on x_i by x_j due to resource competition. The hidden interactions can be graphically represented by a negative edge $\dashv$ from x_j to x_i if $C < 0$, and a positive edge $\rightarrow$ if $C > 0$. The hidden interactions of a cascade are drawn as an example in Fig. 6(b).

Remark: All hidden interactions are activations for a repression network. This is because (i) $\partial f_i/\partial d < 0$, as can be seen from (33), and (ii) $\partial d/\partial x_j < 0$ as we have shown in (31).

IV. AN EXAMPLE: REPRESSION CASCADES

A. Two-Stage Cascade

Cascade circuits are one of the most common network motifs in both natural and synthetic gene networks [24][25]. Here, we consider a simple two-stage repression cascade (Fig. 6(a)). The cascade is composed of three nodes. In node 1, an external input u_1 regulates the production of gRNA g_1 (i.e., $1 \in \mathcal{I}_1$). In node 2, the dCas9-gRNA complex c_1 regulates the production of gRNA g_2 (i.e., $2 \in \mathcal{I}_2$). In node 3, the dCas9-gRNA complex c_2 regulates the production of protein Y_3 (i.e., $3 \in \mathcal{I}_3$). The structure of this motif can be represented by the interaction graph as $g_1 \dashv g_2 \dashv Y$. According to (33a), (33b) and (33c), this cascade can be described by:

$$\dot{g_1} = u_1 - \theta g_1, \tag{37a}$$

$$\dot{g_2} = \frac{\beta_2}{1 + dg_1/\lambda_2} - \theta g_2, \tag{37b}$$

$$\dot{Y_3} = \frac{\beta_3}{1 + dg_2/\lambda_3} - \delta Y_3. \tag{37c}$$

The hidden interactions resulting from the resource competition are illustrated in Fig. 6(b). In this example, we demonstrate that when $c_i \gg Q_i$, $\bar{Y_3}$ adapts perfectly to resource fluctuation. From [21], we know that $Q_i \approx 0.5\text{nM}$. The assumption that $c_i \gg Q_i$ is equivalent to $\lambda_i \ll dg_i$, since $c_i = dg_i/K_i$. Therefore, when $c_i \gg Q_i$, the system dynamics is reduced to:

$$\dot{g_1} = u_1 - \theta g_1, \qquad \dot{g_2} = \frac{\beta_2 \lambda_2}{dg_1} - \theta g_2, \quad \dot{Y_3} = \frac{\beta_3 \lambda_3}{dg_2} - \delta Y_3.$$

The steadt state concentration satisfy:

$$\bar{g_1} = \frac{u_1}{\theta}, \quad \bar{g_2} = \frac{\beta_2'}{\bar{g_1} d}, \quad \bar{Y_3} = \frac{\beta_3'}{\bar{g_2} d},$$

where $\beta_2' = \beta_2 \lambda_2/\theta$, $\beta_3' = \beta_3 \lambda_3/\delta$. Note that by substituting $\bar{g_2}$ into $\bar{Y_3}$, $\bar{Y_3}$ is independent of d.

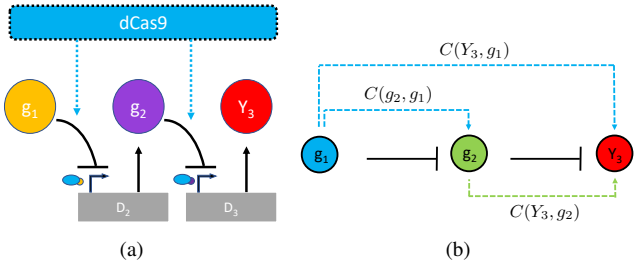

Fig. 6. A CRISPRi 2-stage cascade. (a) Genetic circuit diagram (b) Interaction graph: solid lines represent the intended regulatory interactions; dashed lines represent the hidden interactions due to the resource competition effect.

B. N-Stage Cascade

For a three-stage cascade, perfect adaptation of output to resource competition can not be achieved with the same assumption $c_i \ll Q_i$. Fig. 7 shows how different amounts of resources affect the system behavior. In particular, when resources are abundant, the steady state I/O response is a monotonically decreasing function as expected. As resources become limited, the steady state I/O response becomes biphasic.

The previous two examples demonstrated that resource competition effect depends on circuit's topology. For an N-stage cascade, it is composed of $N+1$ nodes. In node 1, an external input u_1 regulates the production of gRNA g_1. In node i, where $i = 2, \cdots, N$, the dCas9-gRNA complex c_{i-1} regulates the production of gRNA g_i (i.e., $i \in \mathcal{I}_2$). In node $N+1$, the dCas9-gRNA complex c_N regulates the production of protein Y_{N+1}. Under the assumption that $c_i \gg Q_i$, for all $i = 1, 2, \cdots, N$, the dynamics of the system can be written as:

$$\dot{g_1} = u_1 - \theta g_1, \; \dot{g_j} = \frac{\beta_j}{dg_{j-1}} - \theta g_j, \; \dot{Y}_{N+1} = \frac{\beta_{N+1}}{dg_N} - \delta Y_{N+1}.$$

where $j = 2, 3 \cdots, N$. From the dynamics of repression cascades described above, the steady state output concentrations of even-stage and odd-stage cascades are:

$$Y_{N+1} = \begin{cases} \Lambda \bar{g_1}, & \text{if } N \text{ is even}, \\ \frac{\Omega}{\bar{g_1} d}, & \text{if } N \text{ is odd}, \end{cases}$$

where

$$\Lambda = \frac{\beta_3' \beta_5' \cdots \beta_{N+1}'}{\beta_2' \beta_4' \cdots \beta_N'}, \quad \Omega = \frac{\beta_2' \beta_4' \cdots \beta_{N+1}'}{\beta_3' \beta_5' \cdots \beta_N'},$$

and $\beta_k' = \beta_k \lambda_k/\theta$ for all k. We conclude that perfect adaptation to resource competition can be achieved in even-stage cascades since $\bar{Y}_{N+1}$ is independent of free resource concentration (d). For odd-stage cascades, on the other hand, the output concentration at steady state $\bar{Y}_{N+1}$ depends on d. Therefore, when designing cascades in CRISPR-based regulation networks, even-stage cascades may be preferable to odd-stage ones.

V. DISCUSSION AND CONCLUSIONS

CRISPR-based transcription factors provide an exciting alternative to synthetic TF designs due to their ease of use and efficiency in regulating multiple genes in parallel. With CRISPR regulators, multiple endogenous genes can even be regulated to control a complex phenotype, such

Preprint submitted to 57th IEEE Conference on Decision and Control.
Received March 15, 2018.

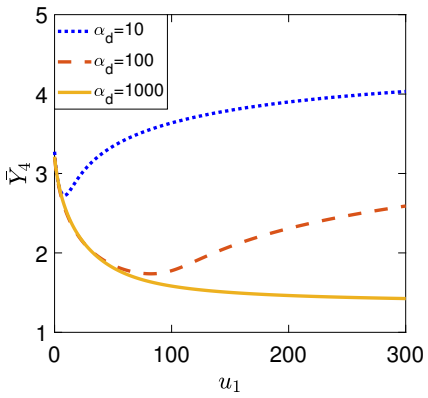

Fig. 7. When there are sufficient resources, the steady state output monotonically decreases as the input is increased. The red line and blue line show that as u_1 increases, the limiting resource results in an opposite effect on steady state output Y. The parameters used here include $D_{1t} = D_{2t} = D_{3t} = 10\text{nM}$, $K_1 = K_2 = K_3 = 0.01\text{nM}$, $Q_1 = Q_2 = Q_3 = 0.5\text{nM}$, $\delta = 1\text{hr}^{-1}$, $\theta = 100\text{hr}^{-1}$, $\kappa_1 = \kappa_2 = 10\text{hr}^{-1}$, $\kappa_3 = 1000\text{hr}^{-1}$.

as cell fate [26]. As the complexity of CRISPR-mediated gene regulation networks increases, limited dCas9 becomes a bottleneck. Therefore, it is critical to identify the underlying resource-sharing mechanism consequence. In this paper, We first study a simple parallel network to reveal hidden interactions arising from resource competition. Then we propose a general modeling framework which is applicable to all repression networks. Finally, we use repression cascades as an example of general networks to illustrate that circuits in certain configurations possess a better robustness to the competition effect. In the future, we will examine how CRISPR-mediated gene regulation networks can be designed to be more robust to resource competition effects. The results in this paper is being experimentally validated in our lab.

Acknowledgement: We thank Aaron Dy, Massimo Bellato and Cameron McBride for their helpful discussions.

REFERENCES

[1] A. S. Khalil and J. J. Collins, "Synthetic biology: applications come of age," *Nature Reviews Genetics*, vol. 11, no. 5, pp. 367–379, 2010.

[2] L. S. Qi, M. H. Larson, L. A. Gilbert, J. A. Doudna, J. S. Weissman, A. P. Arkin, and W. A. Lim, "Repurposing crispr as an rna-guided platform for sequence-specific control of gene expression," *Cell*, vol. 152, no. 5, pp. 1173–1183, 2013.

[3] R. R. Beerli and C. F. Barbas, "Engineering polydactyl zinc-finger transcription factors." *Nature biotechnology*, vol. 20, no. 2, pp. 135–41, feb 2002.

[4] Q. Liu, D. J. Segal, J. B. Ghiara, and C. F. Barbas, "Design of polydactyl zinc-finger proteins for unique addressing within complex genomes." *Proc. Nat. Acad. Sci. (USA)*, vol. 94, no. 11, pp. 5525–5530, 1997.

[5] A. J. Bogdanove, S. Schornack, and T. Lahaye, "TAL effectors: Finding plant genes for disease and defense," pp. 394–401, aug 2010.

[6] A. A. Dominguez, W. A. Lim, and L. S. Qi, "Beyond editing: repurposing CRISPRCas9 for precision genome regulation and interrogation," *Nature Reviews Molecular Cell Biology*, vol. 17, no. 1, pp. 5–15, 2015.

[7] L. A. Gilbert, M. H. Larson, L. Morsut, Z. Liu, G. A. Brar, S. E. Torres, N. Stern-Ginossar, O. Brandman, E. H. Whitehead, J. A. Doudna, W. A. Lim, J. S. Weissman, and L. S. Qi, "CRISPR-mediated modular RNA-guided regulation of transcription in eukaryotes," *Cell*, vol. 154, no. 2, pp. 442–451, 2013.

[8] S. Konermann, M. D. Brigham, A. Trevino, P. D. Hsu, M. Heidenreich, Le Cong, R. J. Platt, D. A. Scott, G. M. Church, and F. Zhang, "Optical control of mammalian endogenous transcription and epigenetic states," *Nature*, vol. 500, no. 7463, pp. 472–476, 2013.

[9] D. Bikard, W. Jiang, P. Samai, A. Hochschild, F. Zhang, and L. A. Marraffini, "Programmable repression and activation of bacterial gene expression using an engineered CRISPR-Cas system," *Nucleic Acids Research*, vol. 41, no. 15, pp. 7429–7437, 2013.

[10] J. G. Zalatan, M. E. Lee, R. Almeida, L. A. Gilbert, E. H. Whitehead, M. La Russa, J. C. Tsai, J. S. Weissman, J. E. Dueber, L. S. Qi, and W. A. Lim, "Engineering complex synthetic transcriptional programs with CRISPR RNA scaffolds," *Cell*, vol. 160, no. 1-2, pp. 339–350, 2015.

[11] A. A. Nielsen and C. A. Voigt, "Multi-input CRISPR/Cas genetic circuits that interface host regulatory networks." *Molecular systems biology*, vol. 10, p. 763, 2014.

[12] S. Kiani, A. Chavez, M. Tuttle, R. N. Hall, R. Chari, D. Ter-Ovanesyan, J. Qian, B. W. Pruitt, J. Beal, S. Vora, J. Buchthal, E. J. K. Kowal, M. R. Ebrahimkhani, J. J. Collins, R. Weiss, and G. Church, "Cas9 gRNA engineering for genome editing, activation and repression," *Nature Methods*, vol. 12, no. 11, pp. 1051–1054, 2015.

[13] Y. Liu, Y. Zeng, L. Liu, C. Zhuang, X. Fu, W. Huang, and Z. Cai, "Synthesizing AND gate genetic circuits based on CRISPR-Cas9 for identification of bladder cancer cells." *Nature communications*, vol. 5, p. 5393, 2014.

[14] Y. Qian, H. H. Huang, J. I. Jiménez, and D. Del Vecchio, "Resource Competition Shapes the Response of Genetic Circuits," *ACS Synthetic Biology*, vol. 6, no. 7, pp. 1263–1272, 2017.

[15] A. Gyorgy, J. I. Jiménez, J. Yazbek, H. H. Huang, H. Chung, R. Weiss, and D. Del Vecchio, "Isocost Lines Describe the Cellular Economy of Genetic Circuits," *Biophysical Journal*, vol. 109, no. 3, pp. 639–646, 2015.

[16] C. McBride and D. Del Vecchio, "Analyzing and exploiting the effects of protease sharing in genetic circuits," in *Proceedings of the 20th World Congress of International Federation of Automatic Control (IFAC)*, Toulouse, France, 2017, pp. 11 411–11 418.

[17] A. Prindle, J. Selimkhanov, H. Li, I. Razinkov, L. S. Tsimring, and J. Hasty, "Rapid and tunable post-translational coupling of genetic circuits," *Nature*, vol. 508, no. 7496, pp. 387–391, 2014.

[18] U. Alon, *An introduction to systems biology : design principles of biological circuits.*, ser. Chapman & Hall/CRC mathematical and computational biology series: 10. Boca Raton, FL : Chapman & Hall/CRC, c2007., 2007.

[19] D. Del Vecchio and R. M. Murray, *Biomolecular Feedback Systems*. Princeton: Princeton University Press, 2014.

[20] A. V. Wright, S. H. Sternberg, D. W. Taylor, B. T. Staahl, J. A. Bardales, J. E. Kornfeld, and J. A. Doudna, "Rational design of a split-Cas9 enzyme complex," *Proc. Nat. Acad. Sci. (USA)*, vol. 112, no. 10, pp. 2984–2989, 2015.

[21] S. H. Sternberg, S. Redding, M. Jinek, E. C. Greene, and J. A. Doudna, "DNA interrogation by the CRISPR RNA-guided endonuclease Cas9," *Nature*, vol. 507, p. 62, jan 2014.

[22] S. E. Clamons and R. M. Murray, "Modeling dynamic transcriptional circuits with crispri," *bioRxiv*, 2017.

[23] W. Rudin, *Principles of mathematical analysis*, 3rd ed. McGraw-Hill, 1976.

[24] S. Kiani, J. Beal, M. R. Ebrahimkhani, J. Huh, R. N. Hall, Z. Xie, Y. Li, and R. Weiss, "CRISPR transcriptional repression devices and layered circuits in mammalian cells," *Nature Methods*, vol. 11, no. 7, pp. 723–726, 2014.

[25] L. Nissim, S. D. Perli, A. Fridkin, P. Perez-Pinera, and T. K. Lu, "Multiplexed and Programmable Regulation of Gene Networks with an Integrated RNA and CRISPR/Cas Toolkit in Human Cells," *Molecular Cell*, vol. 54, no. 4, pp. 698–710, 2014.

[26] N. A. Kearns, R. M. J. Genga, M. S. Enuameh, M. Garber, S. A. Wolfe, and R. Maehr, "Cas9 effector-mediated regulation of transcription and differentiation in human pluripotent stem cells," *Development*, vol. 141, no. 1, pp. 219–223, 2014.